

## Research Article

# Investigation of CO<sub>2</sub>-Sorption Characteristics of Readily Available Solid Materials for Indoor Direct Air Capturing

Lukas Baus,<sup>1</sup> Sascha Nehr ,<sup>1</sup> and Nobutaka Maeda <sup>2</sup>

<sup>1</sup>CBS International Business School, Brühl, Germany

<sup>2</sup>Institute of Materials and Process Engineering (IMPE), School of Engineering (SoE), Zurich University of Applied Sciences (ZHAW), Winterthur CH-8400, Switzerland

Correspondence should be addressed to Sascha Nehr; [s.nehr@cbs.de](mailto:s.nehr@cbs.de)

Received 16 December 2022; Revised 2 March 2023; Accepted 28 June 2023; Published 14 July 2023

Academic Editor: Ting Zhen Ming

Copyright © 2023 Lukas Baus et al. This is an open access article distributed under the Creative Commons Attribution License, which permits unrestricted use, distribution, and reproduction in any medium, provided the original work is properly cited.

Direct air capturing (DAC) is an energy demanding process for CO<sub>2</sub>-removal from air. Ongoing research focuses on the potential of indoor air as DAC-feed to profit from currently unused energetic synergies between DAC and the built environment. In this work, we investigated the performance of three different readily available, solid DAC-adsorbers under typical indoor environmental conditions of 16–25°C, 25–60% relative humidity (RH), and CO<sub>2</sub>-concentrations of less than 800 ppm above atmospheric concentrations. The measured mass-specific CO<sub>2</sub>-adsorption capacities of K<sub>2</sub>CO<sub>3</sub>-impregnated activated carbon, polyethylenimine-snow (PEI-snow), and polyethylenimine (PEI) on silica amount to  $6.5 \pm 0.3 \text{ mg g}^{-1}$ ,  $52.9 \pm 4.9 \text{ mg g}^{-1}$ , and  $56.9 \pm 4.2 \text{ mg g}^{-1}$ , respectively. Among the three investigated adsorber materials, PEI on silica is the most promising candidate for DAC-applications as its synthesis is rather simple, the CO<sub>2</sub>-desorption is feasible at moderate conditions of about 80°C at 100 mbar, and the competing co-adsorption of water does not strongly affect the CO<sub>2</sub>-adsorption under the investigated experimental conditions.

## 1. Introduction

With a global demand for carbon embedded in organic chemicals and derived materials on the order of Mt yr<sup>-1</sup> and a global consumption of fossil carbon on the order of Gt yr<sup>-1</sup>, carbon plays a central role in the industrial value chain both for the production of bulk and fine chemicals and as energy carrier for incineration processes [1, 2]. Thus, carbon represents a cornerstone of the global economy [3]. However, because of increasing concerns related to global warming, the way of carbon utilization must radically change. Current industrial processes lead to enormous amounts of carbon being released into the atmosphere as carbon dioxide (CO<sub>2</sub>). On a global scale, CO<sub>2</sub> impacts the Earth's radiative balance by absorbing radiation in the infrared region and is thereby the main course of man-made climate change. While carbon utilization allowed humanity to thrive for many centuries, it has now become one of the major environmental threats. Numerous national economies agreed on drastic measures to become climate neutral by 2050 [4].

Climate neutrality requires “net zero emissions.” Net zero emissions must be achieved by an overall balance between CO<sub>2</sub>-emissions and CO<sub>2</sub>-sinks. Negative emissions, meaning the active removal of CO<sub>2</sub> from the atmosphere, are necessary and urgently needed to encounter climate change.

Negative emission technologies comprise natural and technical approaches. One natural pathway is global reforestation to enhance the CO<sub>2</sub>-sequestration by photosynthesis [5, 6]. Another pathway resorts to CO<sub>2</sub>-sequestration using crops or even algae and subsequent carbonization of the produced biomass [7, 8]. While undoubtedly necessary, these strategies alone are not capable of removing the vast amount of CO<sub>2</sub> present in the Earth's atmosphere [9]. Moreover, these approaches imply a target conflict regarding the land use for growing either food crops or fuel crops.

A further aspect to be tackled when encountering climate change is industry's immense carbon demand. While mankind might be able to become widely independent from carbon as energy carrier for stationary or mobile combustion processes under certain circumstances, the chemical

industry cannot simply abdicate carbon. Even in 2050, carbon will be required as chemical building block for the production of various chemicals, materials, and pharmaceutical products. In 2021, the production of global crude oil was  $4.5 \cdot 10^{12}$  kg [10]. Considering a simplified sum formula  $(\text{CH}_2)_n$ , this amounts to approximately  $3.8 \cdot 10^{12}$  kg carbon that needs to be saved or replaced in a defossilized scenario.

To date, two major technical pathways are discussed to ensure the carbon feedstock for the chemical and pharmaceutical industry. One technology is postcombustion capturing, where  $\text{CO}_2$  is stripped from rich gas streams such as power plant exhausts or biogas. This process is relatively cost-effective due to the high  $\text{CO}_2$ -concentration in the exhaust streams (typically 5-20%) [11, 12]. However, the largest drawback is the decreasing availability of  $\text{CO}_2$ -rich exhaust streams in the future due to planned shutdowns of power plants operated with fossil fuels. Additionally, the increasing global demand for locally produced food crops as well as the necessity for land use planning to maintain biodiversity will compete with required land use for the production of fuel crops and thus with the production of biogas [13, 14]. The second technology is direct air capturing (DAC) which has been emerging in the past several years. The concept is to capture  $\text{CO}_2$  directly from the atmosphere or air streams similar to atmospheric composition [15]. The major concern here is the high energy demand due to the fact that  $\text{CO}_2$  is filtered at a very low concentration in the range of only 400-1000 ppm. However, several working groups were able to show that there is potential to lower the energy demand by either optimizing the capturing process itself or integrating it into a suitable environment [16–20]. To date, major limitations for using DAC on a large scale for  $\text{CO}_2$ -separation are large mass-specific energy demands of several MWh t<sup>-1</sup>/t  $\text{CO}_2$  [21], large investment costs for  $\text{CO}_2$ -adsorber material, and the availability of suitable upstream and downstream technologies that create co-benefits by using DAC in sector-coupling applications.

In a preceding study, we investigated several potential benefits of incorporating DAC into heating, ventilation, and air conditioning systems (HVAC systems). We outlined that the building's energy demand can be significantly lowered if  $\text{CO}_2$  is stripped from building exhaust air, followed by the partial recirculation of the  $\text{CO}_2$ -depleted and further purified air into the building. This lowers the energy demand for HVAC systems because less ambient air has to be conditioned to meet indoor requirements. We furthermore pointed out that purified recirculated air can be even of higher quality due to reduced intake of outdoor pollutants such as ozone, nitrogen oxides, volatile organic compounds, and particulate matter [18].

To take the next step towards realization of a HVAC/DAC-coupling in recirculation mode, we hereby present experimental findings on potential  $\text{CO}_2$ -adsorber materials for Indoor Direct Air Capturing (IDAC). The IDAC-technology comprises the adsorption of  $\text{CO}_2$  in the built environment at conditions specified for the indoor environmental quality of category II laid down in the European Standard EN 16798-1 of 16-25°C, 25-60% relative humidity (RH), and  $\text{CO}_2$ -concentrations of less than 800 ppm above

atmospheric concentrations [22]. Under these conditions, we measured the mass-specific adsorption capacity of selected adsorber materials. Further, we investigated the minimum desorption temperature at a predefined pressure which later is needed to estimate the mass-specific energy demand for  $\text{CO}_2$ -desorption. Complementary parameters such as co-adsorption of water, material handling, and material durability were also qualitatively assessed. Further process parameters for a reliable calculation of energy demands (adsorber heat capacity, adsorption/desorption enthalpy) were not assessed here.

## 2. $\text{CO}_2$ -Adsorber Materials for IDAC

The  $\text{CO}_2$ -adsorber materials for IDAC investigated in this study were selected to enable a reversible  $\text{CO}_2$ -adsorption via a physical or chemical process. Furthermore, the adsorber materials must be readily available for the intended use. Three materials were chosen that fulfil the above-mentioned criteria: (i)  $\text{K}_2\text{CO}_3$ -impregnated activated carbon, (ii) cross-linked polyethylenimine (PEI-snow), and (iii) polyethylenimine supported on silica (PEI on silica).

**2.1.  $\text{K}_2\text{CO}_3$ -Impregnated Activated Carbon.** Activated carbon is a widely used material and outstanding adsorber due to its large surface area. In this study, we investigated a commercially available activated carbon impregnated with a mass fraction of 10%  $\text{K}_2\text{CO}_3$ , a basic salt that increases the ability to adsorb acidic gases such as  $\text{CO}_2$ . The activated carbon was received as a free sample from Carbotech AC GmbH. It is based on steam-activated mineral coal with a BET-surface of 1000 m<sup>2</sup>.

**2.2. Cross-Linked Polyethylenimine (PEI-Snow).** Polyethylenimine (PEI) is a basic amine-based polymer, which is able to reversibly adsorb  $\text{CO}_2$ . However, pure PEI is a highly viscous liquid that needs to be further treated to function as a solid adsorber. Therefore, PEI (molecular weight = 25 kDa, branched, Merck) is cross-linked with 1,1,1-Tris-(hydroxymethyl)-propane-tris-(glycidylether) (TTE, Merck), an oligoepoxide that links the separated PEI-molecules, yielding solid PEI-snow. In this study, we synthesized PEI-snow with a mass fraction of 3 and 6% of TTE-cross-linker, respectively. The synthesis of cross-linked polyethylenimine, which appears as an aqueous gel, is described by Xu et al. [23].

**2.3. Polyethylenimine Supported on Silica (PEI on Silica).** An alternative to chemically cross-linking PEI is to impregnate it onto the surface of a carrier material. In this study, we used PEI (molecular weight = 25 kDa, branched, Merck) on silica with a mass fraction of 40% PEI. The synthesis of PEI on silica is described by Goeppert et al. [24].

## 3. Methodology

The performance of the  $\text{CO}_2$ -adsorber materials was investigated in a test chamber with a volume of  $(812 \pm 10)$  L. The conditions for adsorption experiments were chosen to meet the specifications of the indoor environmental quality of category II laid down in the European Standard EN 16798-1 of

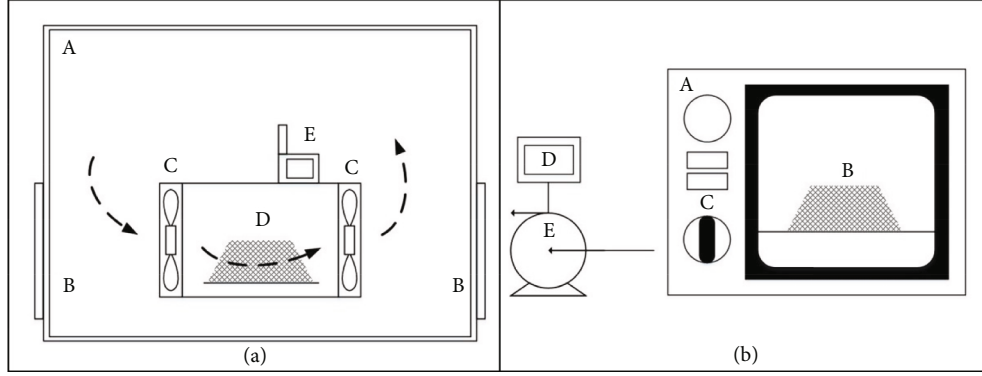


FIGURE 1: Adsorption setup (a) with (A) test chamber corpus, (B) sealable doors, (C) 200 mm fans, (D) adsorber material on paper tray, and (E) sensor for  $T$ ,  $c_{\text{CO}_2}$ , and RH. Dashed arrows indicate the circulating airflow. Desorption setup (b) with (A) vacuum drying cabinet, (B) adsorber material on steel tray, (C) vacuum valve, (D) vacuum control unit, and (E) membrane vacuum pump.

16–25°C, 25–60% RH, and  $\text{CO}_2$ -concentrations of less than 800 ppm above atmospheric concentrations [22]. Most of the experiments presented in the following were conducted under these boundary conditions with few marginal exceptions. At the beginning of each adsorption experiment, the test chamber was conditioned to a defined  $\text{CO}_2$ -level using  $\text{CO}_2$  resulting from paraffin incineration. Subsequently, the  $\text{CO}_2$ -adsorber material was exposed to the chamber's atmosphere in a ventilation channel using two electric fans with an electrical power of 2 W and a diameter of 200 mm, each. Figure 1(a) shows the experimental setup for the adsorption experiments.

All adsorption experiments were carried out for a minimum of three hours after which all materials reached a steady state.  $\text{CO}_2$ -concentration, relative humidity, and temperature were recorded using  $\text{CO}_2$ -sensors (CL-11 NDIR, Rotronic). The  $\text{CO}_2$ -sensors have a declared accuracy of  $\pm 20$  ppm and are equipped with an integrated capacitive hygrometer for the measurement of the relative humidity with a declared accuracy of  $< 2.5\%$  as well as a thermistor for the temperature measurement with a declared accuracy of  $\pm 0.3$  K.

The  $\text{CO}_2$ -adsorption capacity was calculated exclusively based on  $\text{CO}_2$ -concentrations measured in the test chamber according to

$$\Theta_{\text{CO}_2} = \frac{(c_0 - c_1 - c_{\text{leak}}) \cdot \rho_{\text{CO}_2} \cdot V}{m_{\text{ads}}}. \quad (1)$$

$\Theta_{\text{CO}_2}$  denotes the  $\text{CO}_2$ -adsorption capacity in  $\text{mg g}^{-1}$  of the respective material ( $\text{mg CO}_2$  per g adsorber material).

$c_0$  is the initial  $\text{CO}_2$ -concentration in ppm when the adsorber is first exposed to the test atmosphere.

$c_1$  is the final  $\text{CO}_2$ -concentration in ppm after 3 hours of adsorber exposure.

$c_{\text{leak}}$  is the  $\text{CO}_2$ -concentration loss in ppm in the test chamber caused by leakages, calculated using Equation (3).

$\rho_{\text{CO}_2}$  is the density of  $\text{CO}_2$  under STP conditions ( $1.98 \text{ kg m}^{-3}$ ).

$V$  is the test chamber's volume of  $0.812 \text{ m}^3$  (geometrically calculated,  $\pm 0.01 \text{ m}^3$ ).

$m_{\text{ads}}$  is the mass of adsorber used for the experiment.

The test chamber showed an unavoidable leakage, which was considered in the data evaluation. Therefore, some experiments were prolonged overnight. The steady decline of the recorded  $\text{CO}_2$ -concentration after achieving adsorber saturation was used to calculate the leakage for the experiment using

$$k_{\text{leak}} = \frac{\ln(c_3 - c_{\text{out}} / c_2 - c_{\text{out}})}{t_{\text{end}} - t_{\text{start}}}. \quad (2)$$

$k_{\text{leak}}$  is the leakage rate of the test chamber in  $\text{h}^{-1}$ .

$c_2$  is the  $\text{CO}_2$ -concentration for the leakage measurement in ppm, taken 4 hours after initial adsorber exposition and therefore at least one hour after adsorber saturation is achieved.

$c_3$  is the final  $\text{CO}_2$ -concentration in ppm after the leakage experiment's duration of 6 hours.

$c_{\text{out}}$  is the  $\text{CO}_2$ -concentration outside the test chamber in ppm. This value is recorded at the beginning of each experiment and assumed to be constant.

$t_{\text{start}}$  is the starting time for determination of the leakage rate, recorded 4 hours after initial adsorber exposition.

$t_{\text{end}}$  is the end time for determination of the leakage rate, recorded 10 hours after initial adsorber exposition.

Solving Equation (2) for  $c_2$  and subtracting  $c_3$  yield Equation (3) where  $c_{\text{leak}}$  denotes the  $\text{CO}_2$ -concentration loss in ppm in the test chamber caused by leakages.  $c_{\text{leak}}$  is needed for leakage correction of Equation (1).

$$c_{\text{leak}} = c_2 - c_3 = (c_3 - c_{\text{out}}) \cdot e^{[-k_{\text{leak}} \cdot (t_{\text{end}} - t_{\text{start}})]} + c_{\text{out}} - c_3. \quad (3)$$

During the adsorption experiments, the leakage rate  $k_{\text{leak}}$  was individually calculated eight times. The mean value was found to be  $k_{\text{leak}} = (0.015 \pm 0.01) \text{ h}^{-1}$ . This value was used as a constant leakage factor for all adsorber performance corrections in this study. The mean value of  $k_{\text{leak}} = 0.015 \text{ h}^{-1}$  was used for the determination of  $c_{\text{leak}}$  according to Equation (3). We found that the absolute decrease in  $\text{CO}_2$ -concentration due to passive leakage was  $24.1 \pm 1.1$  ppm, which is on the order of the declared sensor accuracy of  $\pm 20$  ppm.

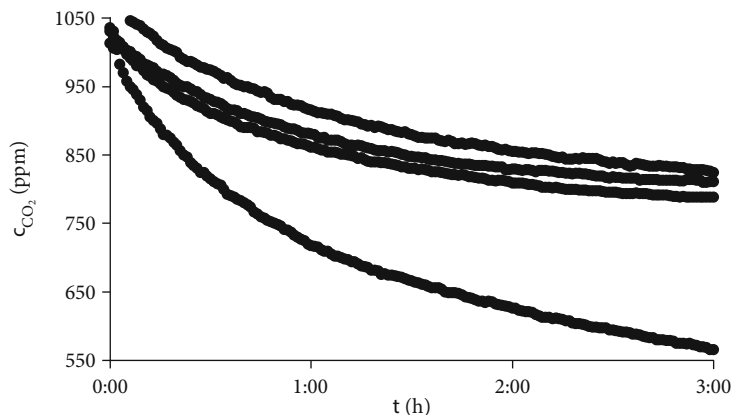


FIGURE 2: Exemplary  $\text{CO}_2$ -adsorption curves for each investigated material. From top to bottom: PEI-snow with a mass fraction of 3% TTE, PEI-snow with a mass fraction of 6% TTE, PEI on silica, and  $\text{K}_2\text{CO}_3$ -impregnated activated carbon. The absolute adsorber performance is no indicator for adsorption capacity as different adsorber masses were used for activated carbon and PEI-based materials, respectively.

The minimum regeneration temperature for the materials was investigated in desorption experiments to achieve complete regeneration when held at this temperature for one hour at 100 mbar. The parameter set consisting of pressure, temperature, and time for regeneration can be further optimized. This issue has not been assessed systematically in this study. Figure 1(b) shows the experimental setup for the desorption experiments. Pressure and regeneration time were kept constant. Pressures below 100 mbar greatly increase the vacuum pump's energy demand and require more effort in future machine design to achieve the necessary tightness. A longer regeneration time increases the thermal stress on the adsorber material, which might affect the durability.

The three materials were compared and evaluated towards their potential for IDAC-applications. Furthermore, potential degradation of the materials due to the thermal stress was qualitatively assessed. Therefore, the  $\text{CO}_2$ -adsorption capacity was compared over all regeneration cycles in which the same batch of the material was used. The mass of the adsorber used for the experiments was selected in a way that the expected  $\text{CO}_2$ -adsorption remains at around 40% ( $\text{K}_2\text{CO}_3$ -impregnated activated carbon) or 20% (PEI-snow and PEI on silica) of the initial  $\text{CO}_2$ -mass in the chamber.

## 4. Results and Discussion

Figure 2 shows exemplary  $\text{CO}_2$ -adsorption curves for each investigated material. Batches of 6 g material were used of PEI-snow and PEI on silica, respectively.  $\text{K}_2\text{CO}_3$ -impregnated activated carbon was used in a 100 g batch.

All materials show a comparable adsorption behavior. When exposed to a  $\text{CO}_2$ -enriched atmosphere, the material adsorbs  $\text{CO}_2$ , resulting in a rapid decline of the  $\text{CO}_2$ -concentration. In the course of the adsorption experiment, the material becomes saturated with  $\text{CO}_2$  while the gas-phase concentration of  $\text{CO}_2$  is reduced. Both effects result in reduced  $\text{CO}_2$ -uptake over time until a steady state is reached. At this point, the measurements start to show a constant decline solely caused by the test chamber's leakage. Figure 3 shows a slow and steady decline of the  $\text{CO}_2$ -concentration in the test chamber exclusively caused by leakage.

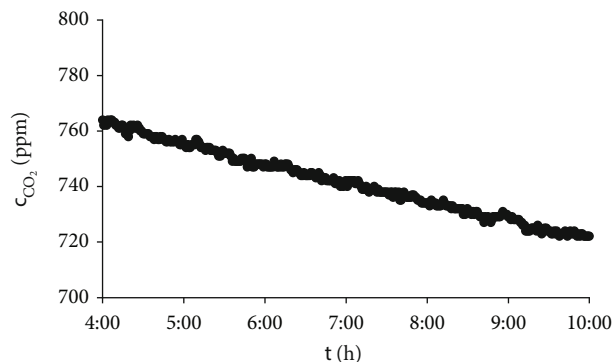


FIGURE 3: Exemplary decay of the  $\text{CO}_2$ -concentration exclusively caused by passive leakage observed 4 to 10 hours after initial adsorber exposition. The regression analysis of the experimental data using Equation (2) yields a leakage rate of  $k_{\text{leak}} = 0.015 \text{ h}^{-1}$  with a determination coefficient of  $R^2 = 0.993$ . The data set shown here was recorded after a regular adsorption experiment with 6 g PEI on silica.

In the following, we present and discuss the experimental results for each investigated  $\text{CO}_2$ -adsorber material for IDAC. The dependence of the  $\text{CO}_2$ -adsorption capacity on the initial  $\text{CO}_2$ -concentration was not systematically investigated in this study.

**4.1.  $\text{K}_2\text{CO}_3$ -Impregnated Activated Carbon.** In general, activated carbon is a robust material. The  $\text{CO}_2$ -adsorption-performance was found to be consistent over the range of experiments. The necessary regeneration temperature at 100 mbar over one hour was found to be  $120^\circ\text{C}$ . Adsorber regeneration at  $100^\circ\text{C}$  leads to a steady decline in  $\text{CO}_2$ -adsorption capacity over three cycles. In contrast, regeneration at  $120^\circ\text{C}$  restored the material's initial  $\text{CO}_2$ -adsorption capacity (cycle 5 in Table 1). In addition to  $\text{CO}_2$ , activated carbon co-adsorbs water as seen in decreasing relative humidity during the experiments. However, no correlation between air humidity and  $\text{CO}_2$ -adsorption capacity was found under the prevailing experimental conditions ranging from 42 to 66% relative humidity over a set of 10 adsorption/

TABLE 1: Experimental results for CO<sub>2</sub>-adsorption on K<sub>2</sub>CO<sub>3</sub>-impregnated activated carbon. Experiments shown here comprise desorption at 120°C, with the exception of cycle 1, which was initially treated at 100°C before first adsorption.

| Starting conditions      |           |           | End conditions           |           |           | Capacity <sup>1</sup><br>(mg g <sup>-1</sup> ) | Cycle <sup>2,3</sup><br># | Capacity corrected <sup>1,4</sup><br>(mg g <sup>-1</sup> ) | Standard dev. <sup>1</sup><br>(mg g <sup>-1</sup> ) |
|--------------------------|-----------|-----------|--------------------------|-----------|-----------|--|---------------------------|--|---|
| CO <sub>2</sub><br>(ppm) | RH<br>(%) | T<br>(°C) | CO <sub>2</sub><br>(ppm) | RH<br>(%) | T<br>(°C) |  |                           |  |   |
| 1018                     | 58.7      | 24.5      | 552                      | 54.5      | 24.2      | 7.5  | 1                         | 7.0  |   |
| 1069                     | 56.9      | 25.2      | 660                      | 46.9      | 25.4      | 6.6  | 5                         | 6.1  | 0.3   |
| 1069                     | 66.0      | 26.2      | 651                      | 51.7      | 25.9      | 6.7  | 6                         | 6.2  |   |
| 1044                     | 51.6      | 23.8      | 596                      | 44.6      | 24.3      | 7.2  | 7                         | 6.7  |   |
| 1055                     | 54.6      | 23.3      | 594                      | 44.7      | 24.4      | 7.4  | 8                         | 6.9  |   |
| 1076                     | 47.7      | 24.3      | 625                      | 43.5      | 24.7      | 7.3  | 9                         | 6.8  | Arithm. mean <sup>1</sup>                           |
| 1021                     | 42.0      | 25.2      | 612                      | 40.1      | 25.9      | 6.6  | 10                        | 6.1  | (mg g <sup>-1</sup> )                               |
| 1070                     | 43.8      | 23.3      | 655                      | 38.5      | 23.9      | 6.7  | 11                        | 6.2  |   |
| 1013                     | 60.7      | 23.1      | 565                      | 44.9      | 23.8      | 7.2  | 12                        | 6.8  | 6.5   |
| 1050                     | 52.2      | 24.1      | 615                      | 42.7      | 24.7      | 7.0  | 13                        | 6.5  |   |

<sup>1</sup>CO<sub>2</sub>-adsorption capacity given in milligram CO<sub>2</sub> per gram adsorber material. <sup>2</sup>Number of adsorption/desorption cycles for this material batch. <sup>3</sup>Missing cycle numbers are not listed here because the corresponding experiments were conducted with different CO<sub>2</sub>-concentrations and/or humidity. <sup>4</sup>CO<sub>2</sub>-adsorption capacity corrected for leakage according to Equation (1).

TABLE 2: Experimental results for CO<sub>2</sub>-adsorption on PEI-snow with a mass fraction of 3% and 6% TTE, respectively. Experiments shown here comprise desorption at three different temperatures.

|        | Starting conditions      |           |           | End conditions           |           |           | Reg. temp.<br>(°C) <sup>5</sup> | Capacity <sup>1</sup><br>(mg g <sup>-1</sup> ) | Cycle <sup>2,3</sup><br># | Cap. corr. <sup>1,4</sup><br>(mg g <sup>-1</sup> ) | Standard dev. <sup>1,6</sup><br>(mg g <sup>-1</sup> ) |
|--------|--------------------------|-----------|-----------|--------------------------|-----------|-----------|---------------------------------|--|---------------------------|--|---|
|        | CO <sub>2</sub><br>(ppm) | RH<br>(%) | T<br>(°C) | CO <sub>2</sub><br>(ppm) | RH<br>(%) | T<br>(°C) |                                 |  |                           |  |   |
| 3% TTE | 1066                     | 50.0      | 22.3      | 816                      | 70.0      | 22.1      | 60                              | 67.1   | 1                         | 58.9   |   |
|        | 1090                     | 44.3      | 22.1      | 872                      | 66.5      | 23.3      | 60                              | 52.9   | 4                         | 44.3   |   |
|        | 1073                     | 51.2      | 22.5      | 883                      | 69.6      | 22.9      | 80                              | 43.5   | 5                         | 35.2   | 4.9   |
|        | 1076                     | 66.8      | 23.7      | 845                      | 75.7      | 23.3      | 100                             | 53.7   | 6                         | 45.3   |   |
|        | 1081                     | 63.0      | 23.5      | 824                      | 76.9      | 23.1      | 100                             | 58.8   | 8                         | 50.3   |   |
| 6% TTE | 1079                     | 57.4      | 25.2      | 718                      | 61.1      | 24.5      | 100                             | 66.5   | 2                         | 58.1   | Arithm. mean <sup>1,6</sup>                           |
|        | 1035                     | 68.3      | 24.3      | 807                      | 74.2      | 25.0      | 100                             | 60.1   | 3                         | 52.3   | (mg g <sup>-1</sup> )                                 |
|        | 1063                     | 59.0      | 24.0      | 815                      | 70.0      | 24.3      | 100                             | 66.6   | 4                         | 58.4   | 52.9  |

<sup>1</sup>CO<sub>2</sub>-adsorption capacity given in milligram CO<sub>2</sub> per gram adsorber material. <sup>2</sup>Number of adsorption/desorption cycles for this material batch. <sup>3</sup>Missing cycle numbers are not listed here because the corresponding experiments were conducted with different CO<sub>2</sub>-concentrations and/or humidity. <sup>4</sup>CO<sub>2</sub>-adsorption capacity corrected for leakage according to Equation (1). <sup>5</sup>Temperature used to regenerate material at 100 mbar for 1 hour prior to adsorption experiment. <sup>6</sup>Standard deviation and arithmetic mean calculated only for experiments with adsorber fully regenerated at 100°C.

desorption cycles. The acquired data is summarized in Table 1.

K<sub>2</sub>CO<sub>3</sub>-impregnated activated carbon shows a comparably (see Table 2 and Table 3) low adsorption capacity for CO<sub>2</sub> of  $6.5 \pm 0.3$  mg g<sup>-1</sup>. However, it is a commercially available product. An increased mass fraction of K<sub>2</sub>CO<sub>3</sub> might even lead to an increased CO<sub>2</sub>-adsorption capacity. Additionally, activated carbon can be yielded from renewable resources such as coconut shells [25, 26]. Furthermore, activated carbon is capable of co-adsorbing water. Obviously, this will increase the energy demand for regeneration since water has to be co-evaporated during the regeneration process. However, co-adsorption of water might be beneficial to lower the additional effort for air dehumidification without additional installations in HVAC systems. Moreover, activated carbon might yield additional co-benefits as it is expected to remove further airborne trace constituents such as particulate matter, volatile organic compounds, and odor-

ous substances. Both air dehumidification and further air purification are process steps in indoor air treatment that often become necessary in partially recirculating HVAC systems. Therefore, impregnated activated carbon can be regarded as a promising material for IDAC.

4.2. *PEI-Snow*. PEI-snow adsorbed on average 52.9 mg CO<sub>2</sub> per g adsorber with a standard deviation of 4.9 mg g<sup>-1</sup>. A correlation between adsorption capacity and TTE-concentration could not be found.

PEI-snow cross-linked with a mass fraction of 3% TTE was tested over several cycles. It was found that the necessary regeneration temperature was 100°C. If regenerated with lower temperature, the CO<sub>2</sub>-adsorption capacity steadily decreases as shown in Table 2 (cycles 1-5). However, the regeneration at 100°C at 100 mbar for 10 minutes resulted in a significant color change of the material from white to yellow. Further regeneration cycles at 100°C

TABLE 3: Experimental results for CO<sub>2</sub>-adsorption on PEI on silica. Experiments shown here comprise desorption at 80°C.

| Starting conditions      |           |           | End conditions           |           |           | Capacity <sup>1</sup><br>(mg g <sup>-1</sup> ) | Cycle <sup>2,3</sup><br># | Capacity corrected <sup>1,4</sup><br>(mg g <sup>-1</sup> ) | Standard dev. <sup>1</sup><br>(mg g <sup>-1</sup> ) |
|--------------------------|-----------|-----------|--------------------------|-----------|-----------|--|---------------------------|--|---|
| CO <sub>2</sub><br>(ppm) | RH<br>(%) | T<br>(°C) | CO <sub>2</sub><br>(ppm) | RH<br>(%) | T<br>(°C) |  |                           |  |   |
| 1010                     | 55.2      | 24.1      | 763                      | 55.8      | 24.6      | 66.3   | 1                         | 58.9   |   |
| 1010                     | 48.4      | 23.1      | 750                      | 50.5      | 24.0      | 69.8   | 3                         | 62.4   |   |
| 1031                     | 49.2      | 25.2      | 788                      | 48.3      | 25.7      | 65.2   | 6                         | 57.5   | 4.2   |
| 1050                     | 49.4      | 25.6      | 821                      | 47.2      | 26.9      | 61.5   | 7                         | 53.5   |   |
| 1019                     | 57.5      | 23.9      | 763                      | 56.4      | 24.8      | 68.7   | 8                         | 61.2   |   |
| 1002                     | 54.4      | 25.3      | 788                      | 54.5      | 26.1      | 57.4   | 9                         | 50.2   | Arithm. mean <sup>1</sup>                           |
| 1067                     | 56.7      | 25.6      | 837                      | 54.4      | 26.9      | 61.7   | 10                        | 53.5   | (mg g <sup>-1</sup> )                               |
| 1031                     | 57.1      | 25.7      | 775                      | 55.4      | 25.8      | 68.7   | 11                        | 61.0   |   |
| 1019                     | 64.1      | 24.9      | 802                      | 58.3      | 25.3      | 58.2   | 12                        | 50.7   |   |
| 1061                     | 41.2      | 25.8      | 821                      | 43.9      | 26.2      | 64.4   | 17                        | 56.3   | 56.9  |
| 1018                     | 45.0      | 24.6      | 763                      | 51.7      | 25.1      | 68.4   | 22                        | 60.9   |   |

<sup>1</sup>CO<sub>2</sub>-adsorption capacity given in milligram CO<sub>2</sub> per gram adsorber material. <sup>2</sup>Number of adsorption/desorption cycles for this material batch. <sup>3</sup>Missing cycle numbers are not listed here because the corresponding experiments were conducted with different CO<sub>2</sub>-concentrations and/or humidity. <sup>4</sup>CO<sub>2</sub>-adsorption capacity corrected for leakage according to Equation (1).

resulted in an intensive orange color. Oxidative decomposition even under reduced pressure of 100 mbar is observed. Orange color might be caused by the formation of nitrogen oxides, potentially through oxidation of amine groups. The loss of the amine groups is expected to lead to the deterioration of CO<sub>2</sub>-adsorption capacity.

The same effect was observed when regenerating PEI-snow with a mass fraction of 6% TTE at 100°C. The material was furthermore found to release a significant amount of water due to evaporation during the adsorption experiments as well as during the regeneration at 100°C. It was not effective to use regenerated and therefore drier material since it showed a significantly reduced CO<sub>2</sub>-adsorption capacity and was not able to resorb water from the test chamber's atmosphere to rehydrate itself. To use the material effectively, it was first regenerated, and distilled water was then added to rehydrate the polymer prior to use for adsorption. The water lost during adsorption results in a significantly increased air humidity within the test chamber as depicted in Table 2.

The necessary regeneration temperature of 100°C and thus the induced thermal stress and inevitable degeneration of the adsorber material hamper a potential usage of PEI-snow for IDAC. To be able to use this material, it might be viable to use hot steam instead of dry air and reduced pressure for regeneration as suggested by Xu et al. [23]. If such regeneration is feasible under certain conditions, PEI-snow might be a promising material that is easily synthesized without waste products.

**4.3. PEI on Silica.** PEI on silica showed comparable CO<sub>2</sub>-adsorption capacities as PEI-snow. The material adsorbed on average 56.9 mg CO<sub>2</sub> per g adsorber with a standard deviation of 4.2 mg g<sup>-1</sup>. However, the material had a smaller influence on air humidity than the other investigated materials.

PEI on silica regenerated at 80°C at 100 mbar for one hour. Under these conditions, no visible degradation occurred during the first ten cycles. Upon further experimenting, a pale yellow color was observed. This might indi-

cate a slow formation of oxidized PEI on the material's surface. However, the material's performance did not significantly change over 22 cycles.

In the range of relative humidity between 40 and 60%, no significant correlation between CO<sub>2</sub>-adsorption capacity and relative humidity was found. However, increasing humidity exceeding 75% led to reduced CO<sub>2</sub>-adsorption capacities in both investigated scenarios with 1000 and 2000 ppm initial CO<sub>2</sub>-load, respectively.

#### 4.4. Comparison of Experimental Results to CO<sub>2</sub>-Adsorption Capacities Reported in Literature.

CO<sub>2</sub>-adsorbers are often grouped for either DAC-application in atmospheric air (about 400 ppm CO<sub>2</sub>) or in a simulated flue gas (5-15% CO<sub>2</sub>). In this study, we report CO<sub>2</sub>-adsorption capacities determined at initial CO<sub>2</sub>-concentrations of about 1100 ppm. Zhang et al. and Leonzio et al. [27, 28] published a list of CO<sub>2</sub>-adsorption capacities for their own and further materials based on PEI or metal organic frameworks (MOFs). The reported mass-specific CO<sub>2</sub>-adsorption capacities range between 3 and 7% for atmospheric air and 6-11% for simulated flue gas. The adsorption capacities found in this work for PEI-based materials fit to the data for atmospheric air capturing. Activated carbon is regularly investigated to capture CO<sub>2</sub> in flue gases or even pure CO<sub>2</sub> atmospheres [29-31]. Mass-specific CO<sub>2</sub>-adsorption capacities of 5-10% in pure CO<sub>2</sub> are documented. However, considering the CO<sub>2</sub>-concentration difference of at least two orders of magnitude as well as the co-adsorption of other species (like, e.g., N<sub>2</sub>), this data is not transferable to a DAC-case as investigated here where we documented a mass-specific CO<sub>2</sub>-adsorption capacity of around 0.7%. Not addressed in this paper, but promising anyway is the material class of MOFs, which have been intensively investigated in the last decade. The flexibility in chemical composition and pore properties renders MOFs to be promising candidates for future DAC applications. However, some basic issues are yet to be overcome such as costs, durability, potential health issues, and tolerance towards humidity [32-34].

**4.5. General Findings.** According to the conducted experiments, we consider PEI on silica to be the most suitable candidate for DAC in the built environment. Looking at necessary chemicals and industrial scale production, PEI is expected to be more expensive than activated carbon in the near future. However, it provides the best combination of durability and CO<sub>2</sub>-capacity under the experimental conditions of this study. The synthesis is rather simple and does not require any complex technical equipment. The necessary regeneration temperature of 80°C is also comparably low and thereby offers potential to reduce the overall energy demand of the IDAC-process. In our setup, we regenerated the loaded adsorber in a vacuum drying cabinet where the adsorber is initially exposed to increased oxidative stress until the reduced desorption pressure of 100 mbar is reached. If the reduced pressure was applied prior to heating or the remaining oxygen was additionally purged out of the vacuum drying cabinet, this oxidative stress might be suppressed in future applications. Alternatively, regeneration time or pressure might be altered to achieve a more sensitive regeneration and thereby increasing the material's durability further. K<sub>2</sub>CO<sub>3</sub>-impregnated activated carbon might play a valuable role in future IDAC-applications as additional adsorber or even additive to use its air-cleaning and moisture-capturing behavior.

## 5. Outlook

There are several additional parameters, which have to be evaluated to assess a material's potential for IDAC. Not only affordability and durability have to be suitable for an endured application. The material's emission behavior has to be known if air is to be recirculated back into a building. This includes the emission of volatile organic compounds, particles, or odors from the material itself or secondary pollutants that might originate from chemical reactions on the material's surface. Additionally, microbial infestation must be prevented, especially when hygroscopic materials are used. Another important issue is the regulatory aspect of realizing IDAC-installations. Indoor air quality is generally evaluated based on its CO<sub>2</sub>-content. IDAC, however, actively reduces the CO<sub>2</sub>-concentration. This might lead to the false assumption of high indoor air quality, although it is in fact loaded with secondary pollutants such as particles, microbial constituents, or volatile organic compounds. To ensure a hygienically harmless indoor air quality, alternative parameters for assessing indoor air quality have to be implemented. Most likely, further air purification technologies have to be used in addition to IDAC to ensure high indoor air quality in a partially recirculated system and to avoid accumulation of pollutants. The evaluation of physical properties and emissions will be subject of further investigations.

Furthermore, IDAC is an energy demanding process. While a certain amount of energy can be saved by recirculating already properly conditioned air back into a building and CO<sub>2</sub> is yielded as valuable product, both factors are currently unlikely to overcome the needed amount of energy for IDAC [18]. It is therefore important to reduce the processes' energy demand by using efficient materials and reactor setups. This

includes compact packaging and realizing low pressure drops for ventilated air as well as an efficient heating of the material itself. Furthermore, a material with low heat capacity would be favorable to reduce the amount of energy needed to heat it up to its regeneration temperature. Beside the process itself, the main energy input has to be optimized. While electricity from the public grid is expensive, on-site generated electricity from solar power or nearby wind turbines might be significantly cheaper [35]. Additionally, waste heat from other processes could be used to preheat the adsorber material for regeneration.

We come to the conclusion that there is indeed potential usage of already available and comparably affordable CO<sub>2</sub>-adsorber materials for IDAC. However, any IDAC-process needs to be optimized towards the active adsorber material as well as to the application, especially when an implementation in the built environment is planned.

## Data Availability

Data is available on request.

## Conflicts of Interest

The authors declare that they have no conflicts of interest.

## Acknowledgments

The authors thank V. Eichenlaub and K. Neumann (Carbotech Gruppe) for providing K<sub>2</sub>CO<sub>3</sub>-impregnated activated carbon. Financial support by the Federal State of North Rhine-Westphalia within the scope of Progres.nrw-Research and by the IMCD Cares Fund is gratefully acknowledged.

## References

- [1] F. Kähler, M. Carus, O. Porc, and C. vom Berg, "Turning off the tap for fossil carbon: future prospects for a global chemical and derived material sector based on renewable carbon," *Industrial Biotechnology*, vol. 17, no. 5, pp. 245–258, 2021.
- [2] P. Friedlingstein, M. O'Sullivan, M. W. Jones et al., "Global carbon budget 2022," *Earth System Science Data*, vol. 14, no. 11, pp. 4811–4900, 2022.
- [3] International Energy Agency, *World Energy Investment 2022*, IEA Publ, 2022.
- [4] European Commission, *European Climate Law - Framework*, 2020.
- [5] United Nations, *New York Declaration on Forests*, 2014.
- [6] J. Busch, J. Engelmann, S. C. Cook-Patton et al., "Potential for low-cost carbon dioxide removal through tropical reforestation," *Nature Climate Change*, vol. 9, no. 6, pp. 463–466, 2019.
- [7] H. Li, T. Ilyina, W. A. Müller, and P. Landschützer, "Predicting the variable ocean carbon sink," *Science Advances*, vol. 5, no. 4, article eaav647, 2019.
- [8] D. J. Farrelly, C. D. Everard, C. C. Fagan, and K. P. McDonnell, "Carbon sequestration and the role of biological carbon mitigation: a review," *Renewable and Sustainable Energy Reviews*, vol. 21, pp. 712–727, 2013.

- [9] T. F. Keenan and C. A. Williams, "The terrestrial carbon sink," *Annual Review of Environment and Resources*, vol. 43, no. 1, pp. 219–243, 2018.
- [10] Statista, *World wide oil production 2021* <https://www.statista.com/statistics/265229/global-oil-production-in-million-metric-tons/>.
- [11] C. H. Yu, C. H. Huang, and C. S. Tan, "A review of CO<sub>2</sub> capture by absorption and adsorption," *Aerosol and Air Quality Research*, vol. 12, no. 5, pp. 745–769, 2012.
- [12] F. Sabatino, A. Grimm, F. Gallucci, M. van Sint Annaland, G. J. Kramer, and M. Gazzani, "A comparative energy and costs assessment and optimization for direct air capture technologies," *Joule*, vol. 5, no. 8, pp. 2047–2076, 2021.
- [13] A. Muscat, E. M. de Olde, I. J. M. de Boer, and R. Ripoll-Bosch, "The battle for biomass: a systematic review of food-feed-fuel competition," *Global Food Security*, vol. 25, article 100330, 2020.
- [14] H. Haberl, K. H. Erb, F. Krausmann, S. Running, T. D. Searchinger, and W. Kolby Smith, "Bioenergy: how much can we expect for 2050?," *Research Letters*, vol. 8, no. 3, 2013.
- [15] N. McQueen, K. V. Gomes, C. McCormick, K. Blumanthal, M. Pisciotto, and J. Wilcox, "A review of direct air capture (DAC): scaling up commercial technologies and innovating for the future," *Progress in Energy*, vol. 3, no. 3, article 032001, 2021.
- [16] J. F. Wiegner, A. Grimm, L. Weimann, and M. Gazzani, "Optimal design and operation of solid sorbent direct air capture processes at varying ambient conditions," *Industrial and Engineering Chemistry Research*, vol. 61, no. 34, pp. 12649–12667, 2022.
- [17] M. Erans, E. S. Sanz-Pérez, D. P. Hanak, Z. Clulow, D. M. Reiner, and G. A. Mutch, "Direct air capture: process technology, techno-economic and socio-political challenges," *Energy & Environmental Science*, vol. 15, no. 4, pp. 1360–1405, 2022.
- [18] L. Baus and S. Nehr, "Potentials and limitations of direct air capturing in the built environment," *Building and Environment*, vol. 208, article 108629, 2022.
- [19] G. C. del Valle-Pérez, J. C. Muñoz-Senmache, P. E. Cruz-Tato, E. Nicolau, and A. J. Hernández-Maldonado, "Carbon dioxide removal from humid atmosphere by a porous hierarchical silicoaluminophosphate/carbon composite adsorbent," *ACS Applied Engineering Materials*, vol. 1, no. 2, pp. 790–801, 2023.
- [20] V. Kulkarni, D. Panda, and S. K. Singh, "Direct air capture of CO<sub>2</sub> over amine-modified hierarchical silica," *Industrial & Engineering Chemistry Research*, vol. 62, no. 8, pp. 3800–3811, 2023.
- [21] M. Fasihi, O. Efimova, and C. Breyer, "Techno-economic assessment of CO<sub>2</sub> direct air capture plants," *Journal of Cleaner Production*, vol. 224, pp. 957–980, 2019.
- [22] *European Committee for Standardization*, EN 16798-1, 2021.
- [23] X. Xu, M. B. Myers, F. G. Versteeg, B. Pejčić, C. Heath, and C. D. Wood, "Direct air capture (DAC) of CO<sub>2</sub> using polyethyleneimine (PEI) "snow": a scalable strategy," *Chemical Communications*, vol. 56, no. 52, pp. 7151–7154, 2020.
- [24] A. Goeppert, M. Czaun, R. B. May, G. K. S. Prakash, G. A. Olah, and S. R. Narayanan, "Carbon dioxide capture from the air using a polyamine based regenerable solid adsorbent," *Journal of the American Chemical Society*, vol. 133, no. 50, pp. 20164–20167, 2011.
- [25] N. Abuelnoor, A. AlHajaj, M. Khaleel, L. F. Vega, and M. R. M. Abu-Zahra, "Activated carbons from biomass-based sources for CO<sub>2</sub> capture applications," *Chemosphere*, vol. 282, article 131111, 2021.
- [26] E. Gallego, F. J. Roca, J. F. Perales, and X. Guardino, "Experimental evaluation of VOC removal efficiency of a coconut shell activated carbon filter for indoor air quality enhancement," *Building and Environment*, vol. 67, pp. 14–25, 2013.
- [27] W. Zhang, H. Liu, C. Sun, T. C. Drage, and C. E. Snape, "Capturing CO<sub>2</sub> from ambient air using a polyethyleneimine-silica adsorbent in fluidized beds," *Chemical Engineering Science*, vol. 116, pp. 306–316, 2014.
- [28] G. Leonzio, O. Mwabonje, P. S. Fennell, and N. Shah, "Environmental performance of different sorbents used for direct air capture," *Sustainable Production and Consumption*, vol. 32, pp. 101–111, 2022.
- [29] J. Yen, L. Lock, H. Ngu et al., "Review of oil palm-derived activated carbon for CO<sub>2</sub> capture," *Carbon Letters*, vol. 31, no. 2, pp. 201–252, 2021.
- [30] C. Pevida, M. G. Plaza, B. Arias, J. Feroso, F. Rubiera, and J. J. Pis, "Applied Surface Science Surface Modification of Activated Carbons for CO<sub>2</sub> Capture," *Applied Surface Science*, vol. 254, no. 22, pp. 7165–7172, 2008.
- [31] M. G. Plaza, C. Pevida, B. Arias, J. Feroso, F. Rubiera, and J. J. Pis, "A comparison of two methods for producing CO<sub>2</sub> capture adsorbents," *Energy Procedia*, vol. 1, no. 1, pp. 1107–1113, 2009.
- [32] J. R. Li, Y. Ma, M. C. McCarthy et al., "Carbon dioxide capture-related gas adsorption and separation in metal-organic frameworks," *Coordination Chemistry Reviews*, vol. 255, no. 15–16, pp. 1791–1823, 2011.
- [33] J. Yu, L. H. Xie, J. R. Li, Y. Ma, J. M. Seminario, and P. B. Balbuena, "CO<sub>2</sub> capture and separations using MOFs: computational and experimental studies," *Chemical Reviews*, vol. 117, no. 14, pp. 9674–9754, 2017.
- [34] M. Klimakow, *Metallorganische Gerüstverbindungen (MOFs), position paper*, DECHEMA Gesellschaft für Chemische Technik und Biotechnologie e.V., 2014.
- [35] D. Lugo-Laguna, A. Arcos-Vargas, and F. Nuñez-Hernandez, "A European assessment of the solar energy cost: key factors and optimal technology," *Sustainability*, vol. 13, no. 6, p. 3238, 2021.